crystals

MDPI

Article

Chromite and Its Thin Kosmochlor and Cr-Omphacite Cortex in Amphibolite from the Myanmar Jadeite Deposits

Yu Zhang, Guanghai Shi * and Jiabao Wen

School of Gemmology, China University of Geosciences (Beijing), Beijing 100083, China; zhangyu@cugb.edu.cn (Y.Z.); 3009230003@email.cugb.edu.cn (J.W.)
* Correspondence: shigh@cugb.edu.cn

Abstract: Chromite in the amphibolites of the Myanmar jadeite deposits has not been well studied. Mineralogical studies on chromite and related kosmochlor and Cr-omphacite in the amphibolite of the Myanmar jadeite deposits were conducted. Compared to the chromite in the adjacent serpentinized peridotite, the chromite had higher Cr_2O_3 (45.67–54.25 wt.%) and MnO (1.82–1.90 wt.%) but lower MgO (1.00–1.96 wt.%) and Al_2O_3 (1.05–15.09 wt.%), similar to the published chromite compositions in jadeitite. Serpentinite was derived from a highly depleted mantle peridotite. There were at least two stages of metasomatism during the transformation of serpentinite + chromite to magnesio-katophorite + chromite + thin kosmochlor (and/or Cr-omphacite cortex). The first stage was the Ca-rich metasomatism of serpentinite, resulting in sodic-calcic amphibole (magnesio-katophorite), which preceded the formation of jadeite. The second stage of Na-rich metasomatism was produced by the Na-Al-Si-rich fluids with the magnesio-katophorite + chromite (contemporaneous with the formation of jadeite). The composition of the fluid was altered by a reaction with magnesio-katophorite, increasing the Ca-Mg content and resulting in the formation of kosmochlor rich in Ca-Mg and/or peripheral Cr-omphacite. This kosmochlor–Cr-omphacite belongs to the Jd-Kos-Di ternary join, which differs from the kosmochlor–Cr-jadeite (which belongs to the Jd-Kos join in jadeitite). The formation of jadeitite with chromite + kosmochlor + Cr-jadeite occurs when large amounts of Na-Al-Si-rich fluids have wrapped the pieces of chromite-bearing amphibolite. This also explains the proverbial "moss spray green" given that amphibole (with chromite) brings out the green color in jadeitite.

Keywords: chromite; kosmochlor; omphacite; Myanmar jadeite deposits

Academic Editor: Sergey V. Krivovichev

Received: 31 December 2024
Revised: 8 January 2025
Accepted: 12 January 2025
Published: 15 January 2025

Citation: Zhang, Y.; Shi, G.; Wen, J. Chromite and Its Thin Kosmochlor and Cr-Omphacite Cortex in Amphibolite from the Myanmar Jadeite Deposits. *Crystals* **2025**, *15*, 79. https://doi.org/10.3390/cryst15010079

1. Introduction

The Myanmar jadeite deposits represent one of the world's largest and most economically important gem-quality jadeitite resources. Myanmar jadeitites and related rocks, as well as the tectonic setting of the Indo-Burma Range (where the jadeite deposits are situated), have attracted much research attention [1–14].

Jadeite ($NaAlSi_2O_6$), a hard and dense clinopyroxene, is formed under high-pressure and low-temperature conditions [1,4,13]. Jadeitite consists predominantly of jadeite or other sodic (-calcic) clinopyroxenes (e.g., omphacite and kosmochlor), together with minor amphibole, albite, and chromite [1,13]. The gem-quality jadeitite (jadeite jade) is collectively called feicui in Chinese. Primary jadeite deposits occur as massive veins cutting serpentinized peridotites in the Myanmar jadeite deposits [7,15,16]. Some veins have a distinct boundary consisting of thin layers of "amphibolites" between jadeitite and serpentinized peridotite [4,11,15,16]. These thin layers have a high amphibole content (up to 70 vol%)

and, notably, lack plagioclase; therefore, they are referred to as amphibole felses [15]. This phenomenon is not found in other jadeitite occurrences worldwide [15].

According to previous geochemical investigations, the occurrence of jadeitite in the world is divided into P-type and R-type [17]. The P-type jadeitite is precipitated from Na-Al-Si-rich fluids in the pores/cracks/fractures of the serpentinite or HP-LT (high-pressure–low-temperature) metamorphic wall rocks during plate subduction [6,15,18–20]. Fluid inclusions (mainly two-phase aqueous) are commonly found in the jadeite core, and rhythmic zoning was observed in euhedral jadeite crystals under cathodoluminescence (CL) and backscattered electron (BSE) imaging [6,15,19–21]. On the other hand, R-type jadeitite is formed by metasomatism and the replacement of plagioclase granite [22], metagabbro [23], or eclogite [17]. The R-type jadeitite partially preserves textural, mineralogical, or geochronological evidence of pre-existing protoliths [23,24].

Textural observations suggest that amphibolite was formed by metasomatic reactions when the Na-Al-Si-rich fluid infiltrated into the jadeitite–serpentinite contact zone under high-pressure conditions [4,15]. The preservation of relict chromite with kosmochlor rims, which occurs in both jadeitite and amphibole felses, indicates a metasomatic origin from a peridotite protolith infiltrated by the Na-Al-Si-rich fluid [5,25–27]. Kosmochlor (ureyite) was first found in iron meteorites [28,29]. Subsequently, terrestrial kosmochlor was reported in the Myanmar jadeite deposits [25,27], Italian Alps [27], the Osayama ultramafic body (Renge metamorphic belt, Japan) [30], and the sludyanka granulite–facies complex (southern Baikal, Russia) [31]. Kosmochlor and other Cr-bearing pyroxenes are widely documented in the Myanmar jadeite deposits, with those of the jadeite-kosmochlor ($NaAlSi_2O_6$-$NaCrSi_2O_6$) composition being the most abundant [5,15,25–27,32]. The relationship between chromite, kosmochlor, and Cr-jadeite in jadeitite has been widely studied, whereas the chromite and kosmochlor in amphibolite are poorly understood.

Here, we analyze the chromite-bearing amphibolite in the Myanmar jadeite deposits and discuss the alteration of chromite and the process and mechanism of the kosmochlor–jadeite–diopside ($NaCrSi_2O_6$-$NaAlSi_2O_6$-$CaMgSi_2O_6$) isomorphism series in amphibolite. Finally, the principle behind the proverbial "moss spray green" phenomenon in jadeitite is explained.

2. Geological Setting

Myanmar is tectonically located between the Qinghai-Tibetan Plateau collisional orogeny and the Sumatra subduction orogeny (Figure 1a). From west to east, it comprises the Indo-Myanmar Range, the West Myanmar block, the Mogu belt, and the Shan Plateau [33–36]. The Myanmar jadeite deposits are exposed in Pharkant-Tawmaw of the Kachin State (northern Myanmar: 25–26° N and 96°12′–96°25′ E) and are geologically located in the northern part of the Central Basin. The area is located between the two ophiolite belts to the east and west and across the western part of the Sagaing fault zone [2,10,33] (Figure 1b).

The jadeite deposits comprise mainly serpentinite mélange, containing jadeitite, glaucophane/mica schist, diopside marble, and amphibolite [7,15,16,36]. The primary jadeitite is mostly white and occurs as massive veins in the Hpakant ultramafic complex (serpentinized peridotite) or as boulders. The jadeitite veins are nearly vertical, N-S trending, 1.5–5 m wide, and 5–100 m long. Some veins have a distinct 3–50 cm wide amphibolite boundary (also known as the amphibolite blackwall) between jadeitite and serpentinized peridotite [11,15,16]. The amphibolites are highly altered, and the alteration products contain residual prismatic amphibole and jadeite. The metamorphic amphibole consists of eckermannite, magnesio-katophorite, nyböite, glaucophane, richterite, and winchite [4,27,37].

Green kosmochlor and Cr-jadeite occur as spherical aggregates or blocks wrapped by amphiboles within or along the amphibolite boundary.

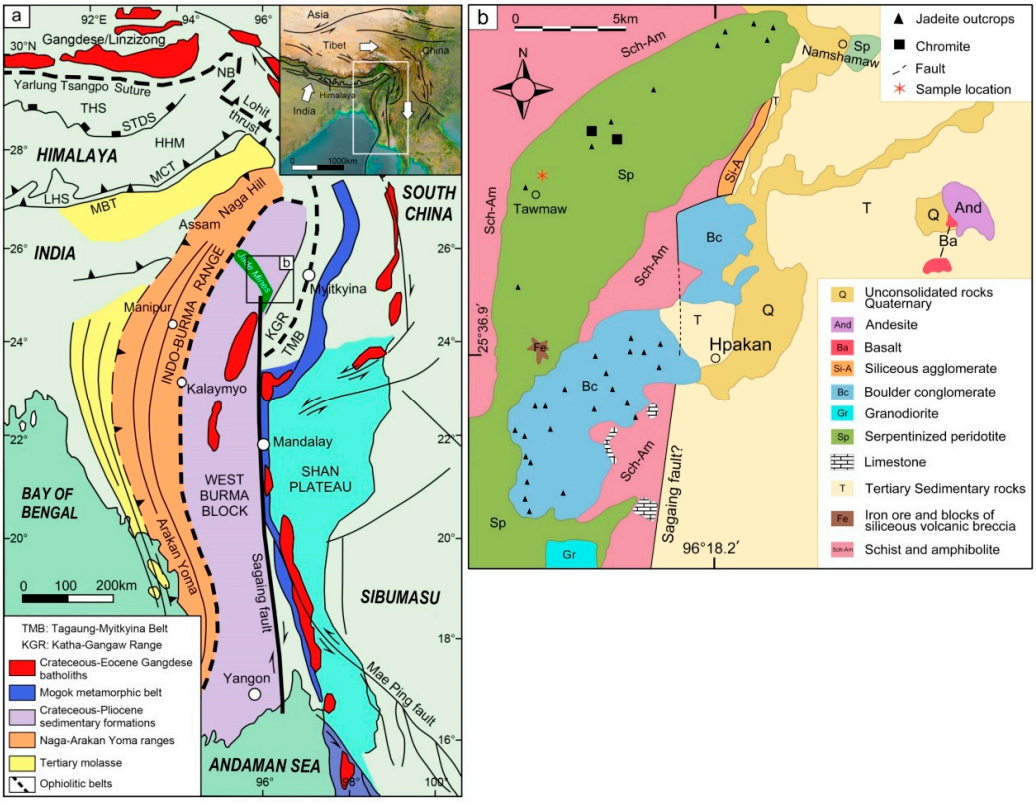

Figure 1. Geological sketch maps of (**a**) Myanmar (modified from [10]) and (**b**) the Myanmar jadeite belt (modified from [7]).

3. Materials and Methods

3.1. Sample Selection and Preparation

Residual black chromite occurs locally and is rimmed by green kosmochlor. We selected three amphibolites with chromite and kosmochlor from the amphibolite boundary in the Myanmar jadeite deposits (Figure 2). The descriptions of the samples are given in Table 1.

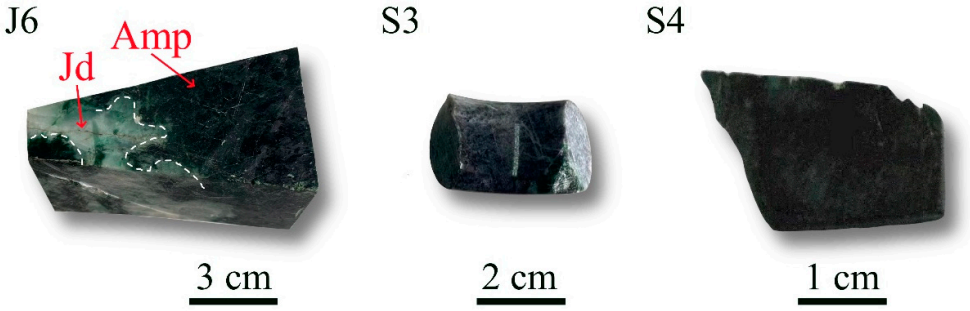

Figure 2. Photos of amphibolite samples with black chromite and green kosmochlor.

All the samples were prepared into polished thin sections (0.03 mm thick) for petrographic observation, electron probe microanalysis (EPMA), micro-X-ray fluorescence (micro-XRF) mapping, and scanning electron microscope (SEM)-BSE imaging.

Table 1. Sample descriptions.

Sample	Rock Type	Mineral Assemblage	Descriptions
S3	Kos-bearing amphibolite	Amp + Chr + Kos + Omp	Main component is black-green amphibole and rounded relict chromite. Reaction with kosmochlor is not obvious.
S4	Kos-bearing amphibolite	Amp + Chr + Kos + Omp + Jd	Granular residual chromite widely disseminated in black-green amphibole. No obvious kosmochlor reaction rim.
J-6	Kos-/Jd-bearing amphibolite	Amp + Chr+ Kos + Jd + Omp	Black-green amphibole in contact with white jadeite. Widespread chromite and fracture-filling green omphacite veinlets in amphibole remain.

Amp: amphibole, Chr: chromite; Kos: kosmochlor; Omp: omphacite; and Jd: jadeite.

3.2. Optical Microscopy

Petrographic observation was performed using an Olympus BX51/DP71 polarizing microscope (manufacturer: Olympus Corporation, Tokyo, Japan) at the laboratory at the School of Gemology, China University of Geosciences (Beijing). We observed the rock microtexture and mineral distribution and assemblage under transmitted and reflected light.

3.3. Micro-XRF Spectrometer

Micro-XRF mapping has the following advantages: it provides rapid and nondestructive in situ testing, has varying area coverage (10s of μm to 10s of cm), and can be used to analyze elemental distribution. A Bruker XRF M4 TORNADO instrument (manufacturer: Bruker Corporation, Karlsruhe, Germany) was used to map the polished thin sections. The mapping used a dual silicon drift detector (SDD), rhodium target and vacuum environment, 20 kV voltage, 300 μA current, and 15 μm pixel step size.

3.4. EPMA and BSE Imaging

The analyses used a JEOL JXA-8100 EPMA (manufacturer: JEOL Corporation, Tokyo, Japan) at the State Key Laboratory of Continental Dynamics, Institute of Geology, Chinese Academy of Geological Sciences. The analysis conditions included a 15 kV acceleration voltage and 2×10^{-8} A beam current. Natural and artificial minerals were analyzed as standard materials. Backscattered electron (BSE) images on the spatial distribution of different minerals were also obtained under the same analysis conditions.

4. Results

4.1. Mineral Content and Texture

The samples mainly consisted of amphibole, which ranged from fine- to coarse-grained (exceeding 200–1000 μm). Amphibole is colorless to pale green under plane-polarized light (PPL) and has a higher interference color (secondary blue to secondary violet) than pyroxenes under cross-polarized light (XPL) (Figure 3). Green kosmochlor occurs as spheroidal or ellipsoidal aggregates (with residual chromite in the core) that have been enveloped by amphiboles (Figure 3a–d). Late jadeite or omphacite veins often filled along the fractures (Figure 3a). Amphibole shows highly deformed fragments at the edges of the junction with large areas of jadeitite (Figure 3e–g).

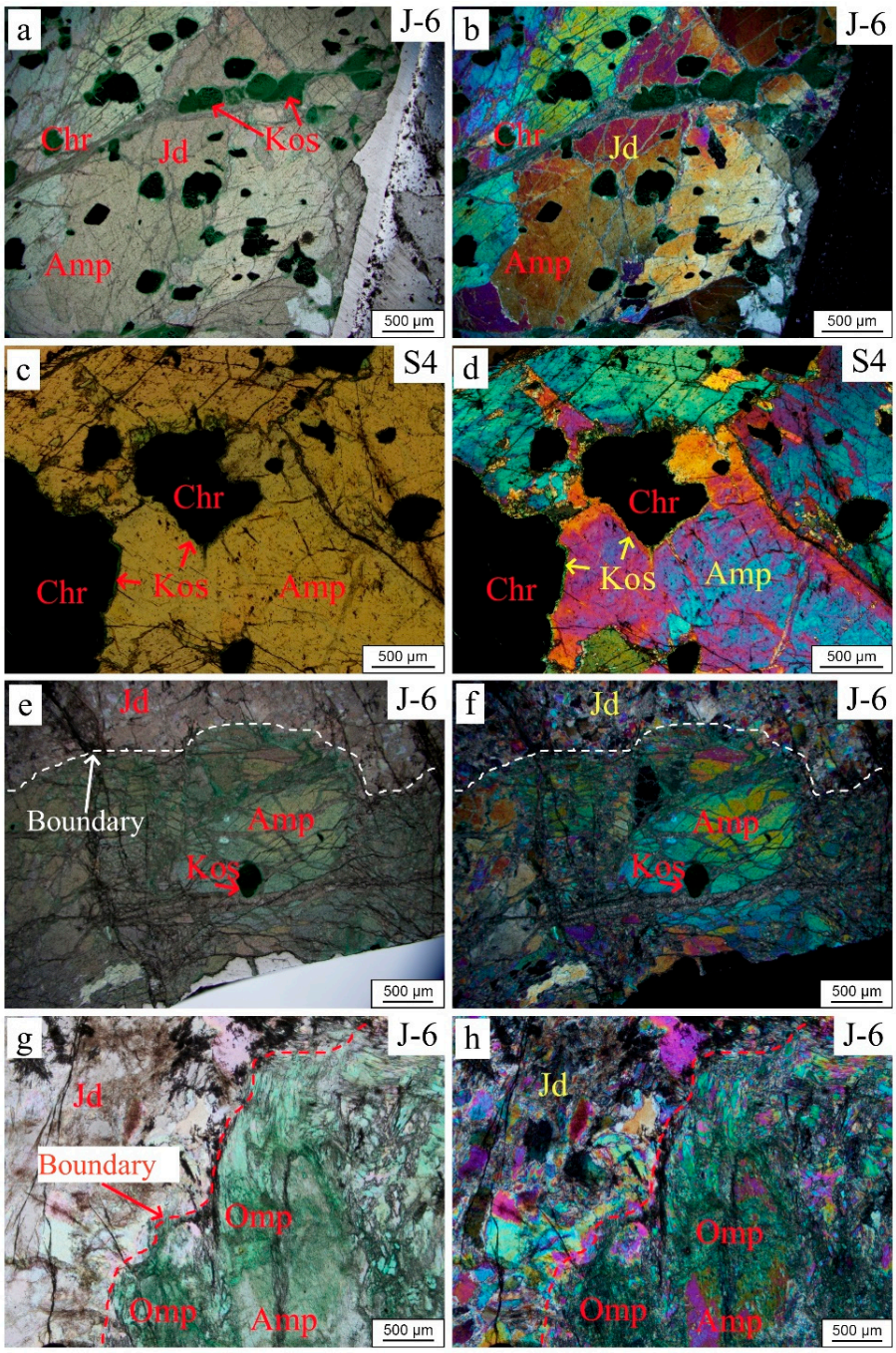

Figure 3. Photomicrographs showing the relationship between amphibole and related minerals. (**a**,**b**): Late jadeite veins filled along the amphibole fractures. (**c**,**d**): Green kosmochlor occurs as spheroidal or ellipsoidal aggregates with residual chromite in the core, which have been enveloped by amphiboles. (**e**–**h**): Highly deformed amphibole fragments at the jadeite boundary (left column: PPL and right column: XPL). Chr: chromite, Jd: jadeite, Omp: omphacite, Kos: kosmochlor, and Amp: amphibole.

Chromite particles are widely scattered in amphibole and can be divided into three groups (chromite-1 to -3), corresponding to three alteration stages. Chromite-1 (J-6-1-4-1a, see Table S1) has a rounded margin and is 10s to 500 μm in size. It is surrounded by a thin kosmochlor rim (J6-1-23a and J6-1-23b) (Figures 3c,d and 4a,b) and has a low degree of alteration. Chromite-2 (S4-103 and S4-105) is highly fragmented and surrounded by kosmochlor (S4-110), with a large Cr-omphacite cortex (S4-112 and S4-113) (Figure 4c,d). Chromite-3 (S4-100 and S4-102) is extremely fine (few to 10 μm) and dispersed in the

omphacite substrate. It is euhedral–subhedral octahedral or granular and is surrounded by a large amount of Cr-omphacite (S4-107) (Figure 4e,f).

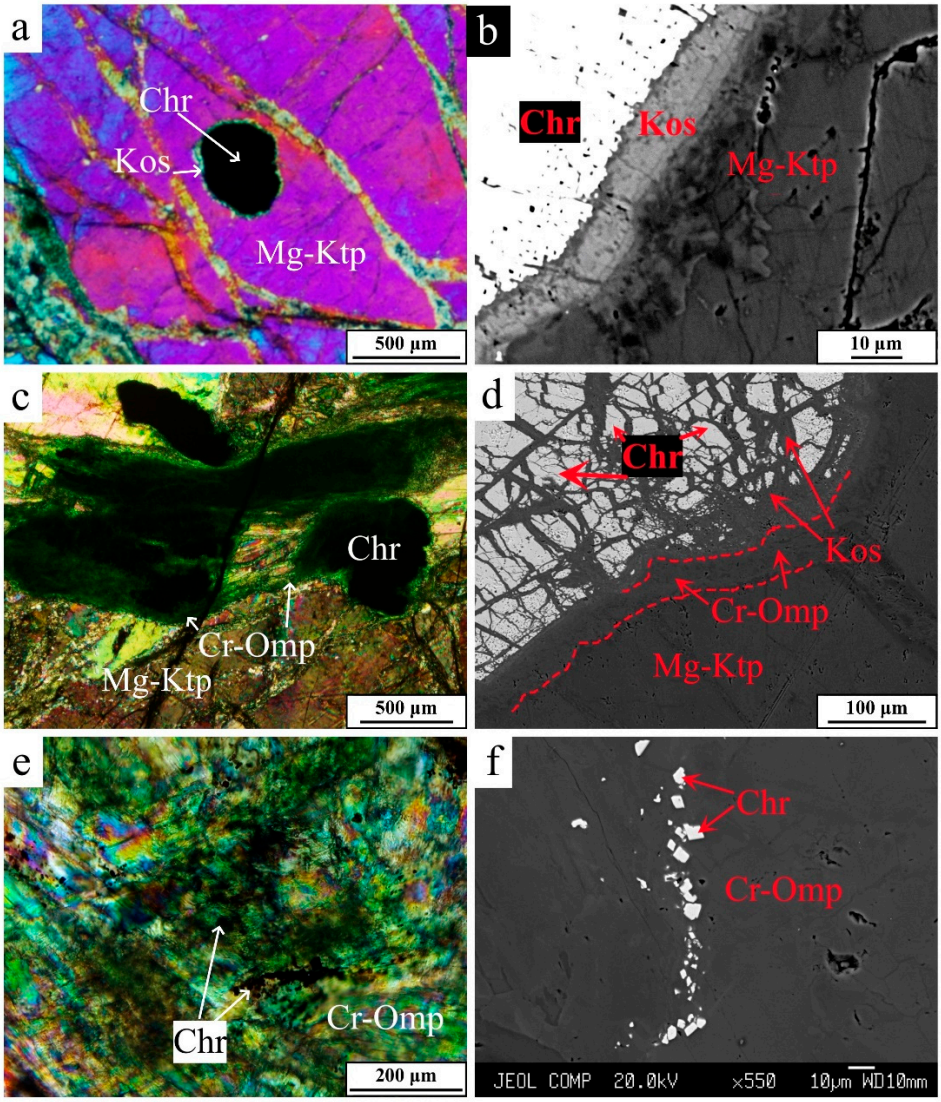

Figure 4. Photographs of three alteration stages of chromite in amphibolite (left column: XPL and right column: PPL): (**a**,**b**) first stage, (**c**,**d**) second stage, and (**e**,**f**) third stage. Chr: chromite, Kos: kosmochlor, and Cr-Omp: Cr-omphacite.

These kosmochlor grains are also different from those found in jadeitite in that (1) they are mostly fine-grained aggregates (few to 10s of μm) (Figures 3 and 4) and (2) the Cr-omphacite cortex (rather than Cr-jadeite) is present in the outer rim of kosmochlor (Figure 4d). In contrast, kosmochlor in jadeitite is often prismatic and fibrous around chromite and surrounded by Cr-jadeite, forming a three-layer chromite–kosmochlor–Cr-jadeite structure [5].

Jadeite occurs at the amphibolite boundary (Figure 3e–h) or as fracture-/cleavage-filling veins in amphibole (Figures 3a,b and 5). The jadeite is mostly euhedral–subhedral prismatic, often with compositional zoning (including an outer omphacite-rich rim) (Figure 5).

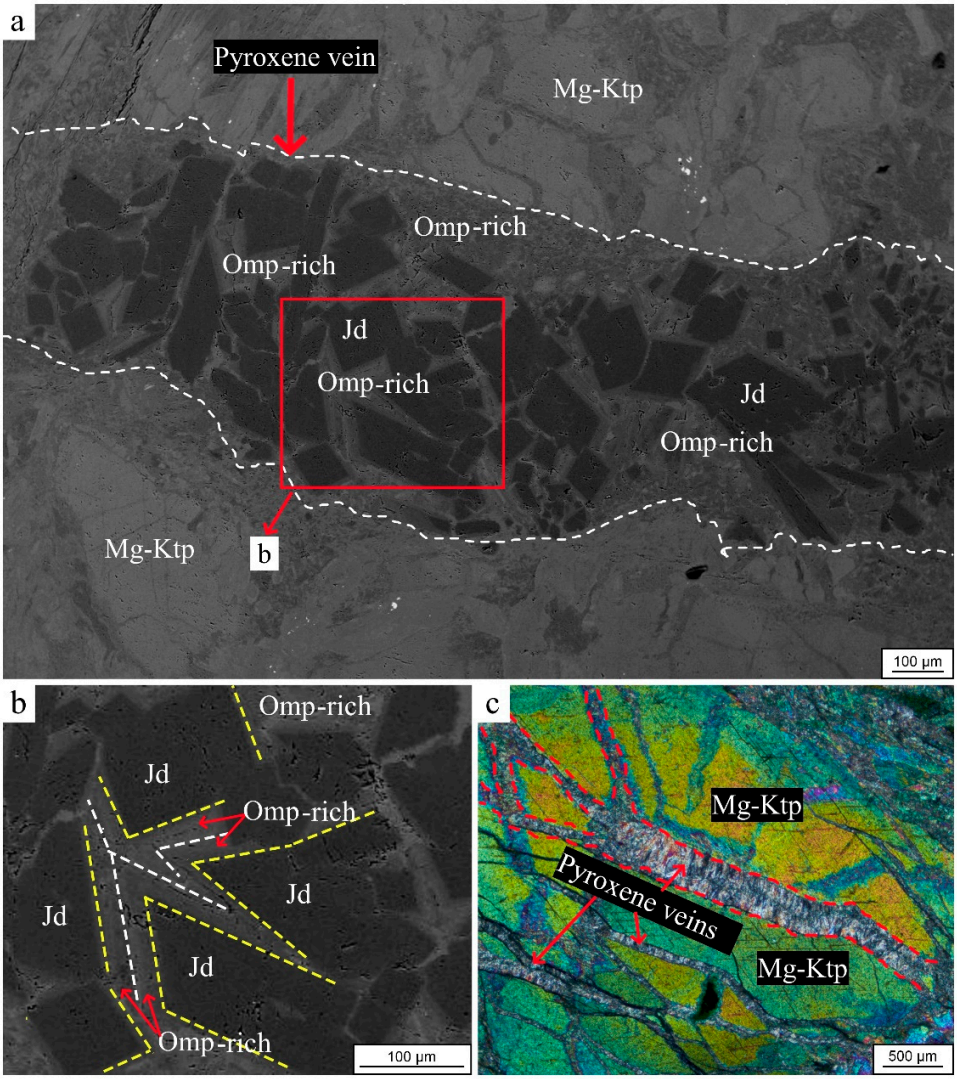

Figure 5. (**a**) BSE image of the pyroxene vein that cut the magnesio-katophorite. Dark color: jadeite (Jd); grey: omphacite-rich jadeite (Omp-rich); and light grey: magnesio-katophorite (Mg-Ktp). (**b**) Jadeite in the vein is euhedral prismatic, often with an outer omphacite-rich rim. (**c**) Pyroxene veins occur as fracture-/cleavage-filling veins in magnesio-katophorite.

4.2. Micro-XRF Mapping

Micro-XRF element maps of sample S4 show that the amphibole is rich in Mg, Ca, and Fe (Figure 6). The chromite mainly contains Fe and Cr, with trace amounts of Al and Mg. The Mg-Ca contents are higher in the fine clinopyroxene veins in amphibolite (S4) than in the white jadeite in contact with the amphibolite (J6).

4.3. Mineral Chemistry

4.3.1. Chromite

The EPMA results indicate that the chromite in the amphibolite samples geochemically mimics the reported chromite composition in jadeitite, featuring high Cr-Mn and low Mg-Al. The chromite consists of 45.67–54.25 wt.% Cr_2O_3, 31.12–33.39 wt.% TFeO (calculated as FeO = 22.27–29.61 wt.%, Fe_2O_3 = 2.52–11.12 wt.%), 1.00–1.96 wt.% MgO, 1.05–15.09 wt.% Al_2O_3, and 1.82–1.90 wt.% MnO. Chromite has high Cr# (69–97) (atomic Cr/[Cr + Al] × 100), very low Mg# (6–12) (Mg/[Mg + Fe^{2+}] × 100), low Y_{Fe} (Fe^{3+}/[Cr + Al + Fe^{3+}] = 0.03–0.18), and low TiO_2 (0.03–0.05 wt.%) contents (Table S1).

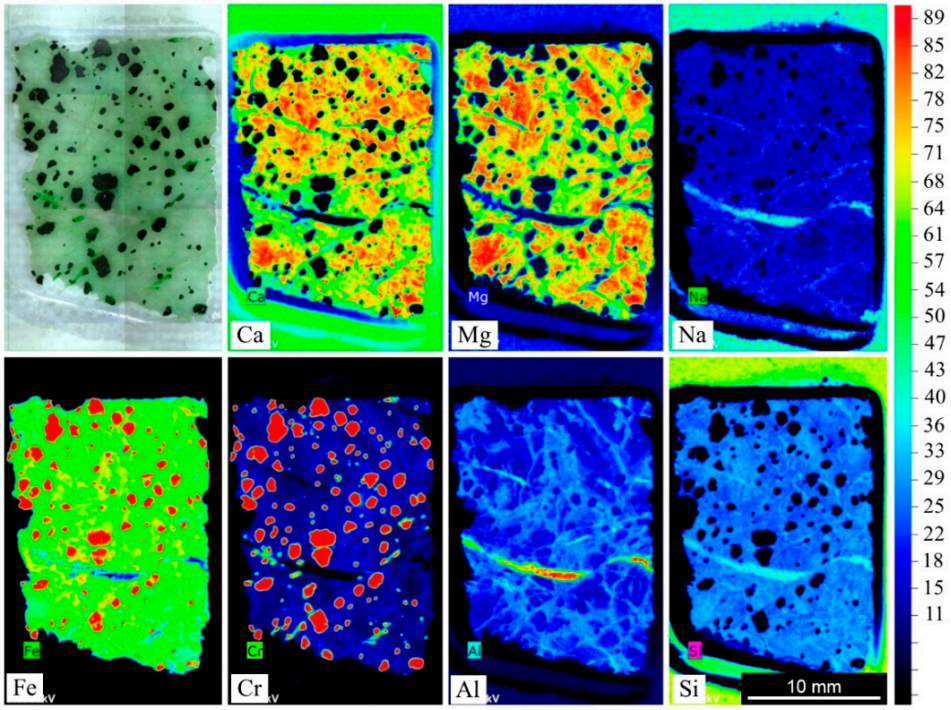

Figure 6. Micro-XRF element maps for Ca, Mg, Na, Fe, Cr, Al, and Si.

4.3.2. Clinopyroxenes (Jadeite, Omphacite, and Kosmochlor)

The clinopyroxenes in our sample were jadeite ($NaAlSi_2O_6$), omphacite, and kosmochlor ($NaCrSi_2O_6$). Omphacite [(Ca, Na) (Mg, Fe^{2+}, Al)Si_2O_6] is composed of a solid solution of jadeite (Jd: $NaAlSi_2O_6$) and diopside (Di: $CaMgSi_2O_6$), with subordinate hedenbergite (Hd: $CaFe^{2+}Si_2O_6$) and aegirine (Ac: $NaFe^{3+}Si_2O_6$) [13,38–40]. The EPMA clinopyroxene data were plotted on the ternary Quad (Wo + En + Fs)-Jd (jadeite)-Ae (aegirine) (where Wo = wollastonite, En = enstatite, Fs = ferrosilite) pyroxene discrimination plot to distinguish jadeite from omphacite (Figure 7).

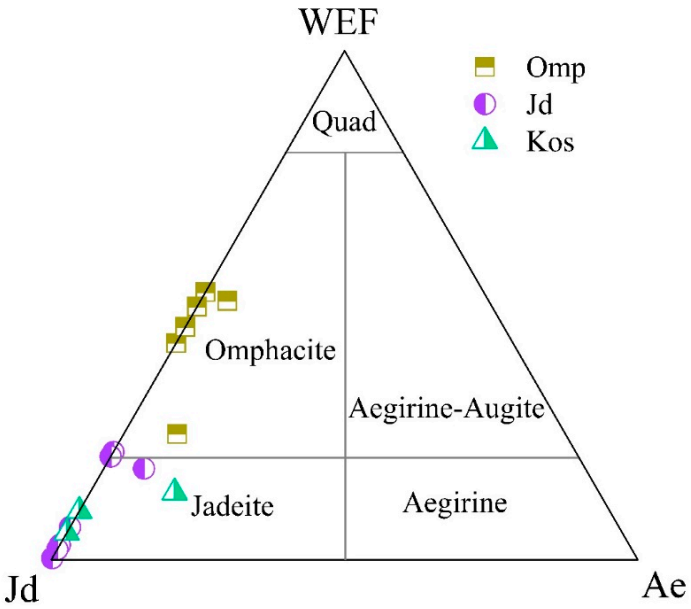

Figure 7. Ternary WEF (Wo + En + Fs)-jadeite (Jd)-aegirine (Ae) classification plot for clinopyroxene in amphibolite (base map from [41]). Quad: quadrilateral pyroxene, i.e., WEF: wollastonite (Wo, $Ca_2Si_2O_6$) + enstatite (En, $Mg_2Si_2O_6$) + ferrosilite (Fs, $Fe_2Si_2O_6$).

However, this cannot distinguish kosmochlor, which is plotted in the jadeite region. We plotted our microprobe analyses using the ternary jadeite–diopside–kosmochlor diagram of Ouyang and Ng (2012) [42] to classify the jadeite and kosmochlor (Figure 8).

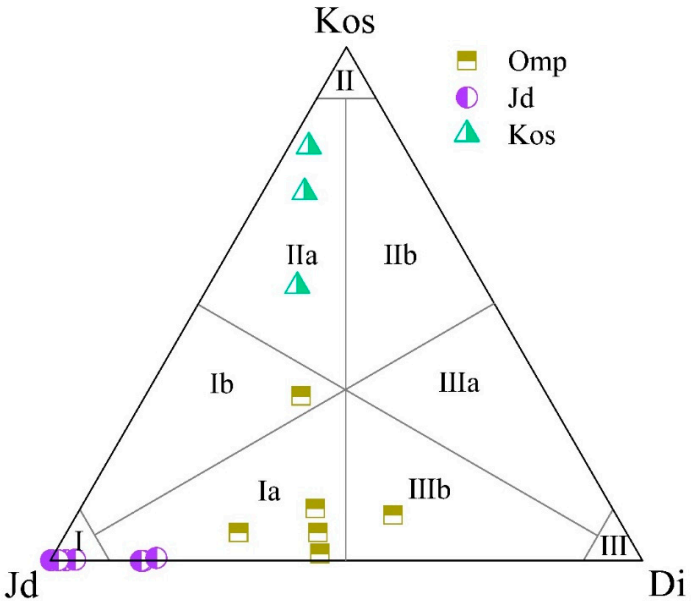

Figure 8. The compositions of Kos-bearing diopside in amphibolite plotted on a Kosmochlor (Kos)-jadeite (Jd)-diopside (Di)-ternary diagram (base map from [42]). The fields define pure jadeite (I), jadeite with minor omphacite (Ia), chromium-containing jadeite (Ib), pure kosmochlor (II), jadeite-containing kosmochlor (IIa), diopside-containing kosmochlor (IIb), pure diopside (III), kosmochlor-containing diopside (IIIa), and jadeite-containing diopside (IIIb).

The chemical composition and classification of clinopyroxenes (including jadeite, kosmochlor, and omphacite) in the amphibolite samples are given in Table S2.

The kosmochlor reaction rim (J6-1-23a and J6-1-23b) around chromite-1 (J-6-1-4-1a) is narrow (~10 μm thick) and has 24.25–27.37 wt.% Cr_2O_3, 1.84–2.23 wt.% TFeO, 0.85–1.77 wt.% CaO, 0.46–1.24 wt.% MgO, and 2.68–3.67 wt.% Al_2O_3. No jadeite was detected. The Cr content of kosmochlor (S4-110) in the chromite-2 (S4-103 and S4-105) grain margin is low, whereas its Ca-Mg content is higher than that of kosmochlor around chromite-1, i.e., the $CaMgSi_2O_6$ component is high (Cr_2O_3 = 15.85 wt.%, CaO = 3.39 wt.%, MgO = 2.74 wt.%, TFeO = 2.56 wt.%, and Al_2O_3 = 7.39 wt.%). The periphery of kosmochlor comprises a thin cortex containing a large amount of Cr-omphacite (S4-112 and S4-113), with 2.89–10.06 wt.% Cr_2O_3, 6.09–8.33 wt.% CaO, 3.98–13.10 wt.% MgO, 3.27–4.34 wt.% TFeO, and 9.35–9.39 wt.% Al_2O_3. Chromite-3 (S4-100 and S4-102) is surrounded by Cr-omphacite (S4-107), with 3.00 wt.% Cr_2O_3, 13.36 wt.% CaO, 8.60 wt.% MgO, 2.77 wt.% TFeO, and 8.99 wt.% Al_2O_3. No kosmochlor was detected.

The chemical composition of the white jadeite in contact with the amphibolite boundary is pure and close to theoretical values (J6-2-7-2 and J6-2-8-2) (Figure 3e–h). In the late fracture-filling veins in the amphibolite, the crystal core is pure jadeite (S4-117 and S4-122), and the outer rim is omphacite-rich jadeite (S4-118, S4-119, and S4-120) (Figure 5). In some finer veins, the main mineral is omphacite (S4-116). Omphacite (J6-2-7-1 and J6-2-8-1, with 0.52–1.99 wt.% Cr_2O_3) also occurs at the edge of broken amphibole (adjacent to pure jadeite).

4.3.3. Amphibole

The amphibole chemical composition and its variability can be expressed by the general formula $AB_2C_5T_8O_{22}W_2$, where:

A = □ (vacancy), Na, K, Ca, and Pb^{2+}
B = Li, Na, Mg, Fe^{2+}, Mn^{2+}, and Ca
C = Li, Mg, Fe^{2+}, Mn^{2+}, Zn, Co, Ni, Al, Fe^{3+}, Cr^{3+}, Mn^{3+}, V^{3+}, Ti^{4+}, and Zr
T = Si, Al, and Ti^{4+}
W = (OH), F, Cl, and O

The chemical compositions and types of the amphiboles are shown in Table S3. According to the amphibole nomenclature adopted by the International Mineralogical Association (IMA) [43], our samples are magnesio-katophorites, which are sodic-calcic amphibole.

Magnesio-katophorite is abundant in the amphibolite blackwall of the Myanmar jadeite deposits [4,26]. In our samples, the magnesio-katophorite consists of 6.97–7.18 apfu Si, 3.52–3.76 apfu Mg (C-site), 1.07–1.31 apfu Ca (B-site), 0.69–0.93 apfu Na (B-site), and 0.77–0.91 apfu Na (A-site).

5. Discussion

5.1. Sources of Jadeitite-Forming Fluids and Magnesio-Katophorite Formation

Solubility experiments related to the blueschist–eclogite transition have shown that dehydration of the hydrated basalt portion of the subducted plate produces Na-Al-Si-rich fluids that can form jadeitite [44]. Compared to mid-ocean ridge basalts (MORBs), Myanmar jadeitite is enriched in Ba, Pb, Sr, U, and Li but is deficient in Rb and K [20,21]. The discovery of deep-sea Type I iron-rich cosmogenic spherules in jadeitite from Myanmar [45], the highly depleted mantle Hf isotopic characteristics of zircons in jadeitite [21,46], and the presence of Ba- and Sr-bearing minerals in jadeitite from Myanmar, Guatemala, and Japan [47–51] suggest that Na-Al-Si-rich fluids may have been derived from seawater, oceanic crust sediments, and dehydration of altered oceanic crust during subduction [20,21,45,46,52,53]. An additional possibility is that these fluids may have been produced from the rodingitization of oceanic mafic rock [54]. In addition, a small amount of serpentinization-derived fluids were involved in the fluids that formed jadeite [11,19,20].

Serpentinite is derived from a highly depleted mantle peridotite [11,21]. The Na-Al-Si-rich fluid precipitated during oceanic subduction in serpentinite cracks produced by tectonic stresses in the forearc mantle wedge, forming the P-type jadeitite [4,5,15,20,55–58]. Concurrently, amphibolite blackwall, being both the spatial and chemical intermediate between jadeitite and serpentinite, was formed through metasomatic reactions as the fluid infiltrated the boundary of the serpentinite cracks [4,15]. The distribution of chromite, jadeitites, amphibolite blackwall, and serpentinite is shown schematically in Figure 9. The white jadeite in contact with the amphibolite boundary is chemically pure and close to theoretical values (J6-2-7-2 and J6-2-8-2) (Figure 3e–h), and it was precipitated from the Na-Al-Si-rich fluid.

The amphiboles in this study are predominantly magnesio-katophorite (a sodic-calcic amphibole), which is very rare in high-P and ultrahigh-pressure rocks, with known occurrences in eclogite from the Western Alps [59], peridotite xenoliths from Marsabit in Kenya [60], and hydrous mantle xenoliths hosted by Pliocene–Quaternary basalts from Yemen [61]. However, it occurs abundantly in the reaction boundaries of jadeitite from the Myanmar jadeite deposits [4,26,37]. The paragenesis of magnesio-katophorite associated with jadeitite has been interpreted as a stage in the progressive metasomatic reaction between jadeite-forming fluids (Na-Al-Si-rich fluids) and serpentinizing peridotite (serpentinite) [37]. The magnesio-katophorites and kosmochlor-bearing diopside are also commonly observed in hydrous mantle xenoliths hosted by Pliocene–Quaternary basalts from Yemen, possibly formed through metasomatism by hydrous Na-rich carbonatite melt [61]. Shi et al. (2003) [4] studied six amphiboles (eckermannite, magnesio-katophorite, nyböite, glaucophane, richterite, and winchite) associated with Myanmar jadeitite and

found that magnesio-katophorite is an early amphibole phase and that Ca decreases and Na increases in the composition of the amphibole as metasomatism develops. The paragenesis of magnesio-katophorite associated with jadeitite is most likely associated with a Ca-rich metasomatism that preceded the formation of jadeitite. The process by which this metasomatism occurred is unclear. However, there is evidence that it occurred.

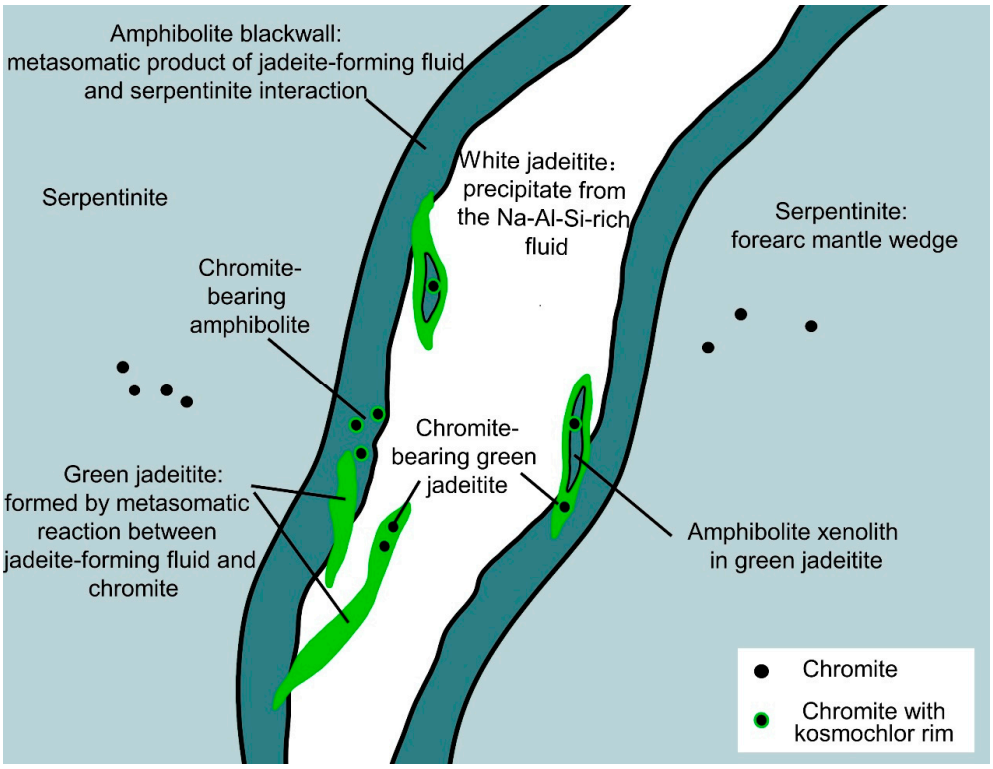

Figure 9. Schematic showing the distribution of chromite, jadeitite, amphibolite blackwall, and serpentinite in the Myanmar jadeite deposits (not to scale). After the initial fracturing of the forearc mantle wedge (perhaps during subduction initiation), the Na-Al-Si-rich fluid infiltrated a fracture zone, resulting in serpentinization of the host peridotite, the formation of amphibolite blackwall and green jadeitite (R-type) along fractures and dyke edges, and the precipitation of white jadeite (P-type) from the Na-Al-Si-rich fluid.

The rare phenomenon of residual chromite cores being directly surrounded by radial uvarovite aggregates, followed by radial kosmochlor aggregates, and then by chromium-bearing jadeite aggregates, has been found in Myanmar jadeitite [15,62]. This phenomenon suggests that Ca-rich metasomatism may have occurred before the formation of kosmochlor and jadeitite [15].

This reaction of evolution from serpentine to magnesio-katophorite can be expressed as:

$$\text{Serpentine} + Ca^{+}_{(aq)} + Na^{+}_{(aq)} + Al^{3+}_{(aq)} + Si^{4+}_{(aq)} \rightarrow \text{Magnesio-katophorite.}$$

5.2. Metasomatism Reaction of Chromite

Chromite is a relic of protolithic peridotite from the subduction channel–mantle wedge and occurs in jadeitite and amphibolite in the Myanmar jadeite deposits [5,25–27]. During jadeite formation, chromite in the serpentinite was subject to infiltration and replacement by jadeite-forming fluids (containing Na, Al, and Si), forming kosmochlor in the chromite rim.

EPMA data show that the residual chromite in amphibolite has lower Al-Mg but higher Cr-Mn contents than the adjacent serpentinized peridotite. A reduction in Mg and

Al contents and an elevation in Cr and Mn contents are observed from chromite-1 to -3, indicating a preferential reaction of the former elements during metasomatism and an increase in the latter elements in the residual chromite. The degree of alteration increases from chromite-1 to -3.

The degree of chromite alteration depends mainly on the fluid–rock ratio [11]. Initially, the chromite-bearing amphibolite reacts with a small amount of fluid and undergoes metasomatism along the margins of the chromite-1 grains, forming a thin kosmochlor rim. More fluid then infiltrates, forming a three-layered structure centered on chromite-2 with kosmochlor and Cr-omphacite. Chromite-2 is also frequently fractured, and kosmochlor replaces chromite along the fracture. Finally, large amounts of fluid exacerbate the breaking of the chromite, leaving only small euhedral chromite-3, and Cr-omphacite completely replaces the surrounding kosmochlor.

The residual chromite in green (kosmochlor-) jadeitite is also similarly altered, but its degree of alteration is generally higher than that of chromite-3. Evidence from MgO content and δ^{26}Mg value in the jadeite formation system shows that jadeite was formed in an open system with a high fluid–rock ratio [11]. With such a high fluid–rock ratio, some chromite-bearing amphibolite was replaced entirely to form green jadeite (which may contain chromite) (Figure 9).

5.3. Formation of Cr-Bearing Pyroxenes (Kosmochlor and Cr-Omphacite)

Cr-bearing pyroxenes (e.g., kosmochlor) are common in jadeite rocks in Myanmar [5,25–27,32]. These Cr-bearing pyroxenes are often developed around chromite. This suggests that this kosmochlor and Cr-jadeite was formed by the replacement of magmatic chromite as a result of Na-rich jadeite-forming fluid under high-pressure conditions (estimated T ≈ 250–370 °C and P ≈ 1–1.2 GPa) [4,5,27,31,32].

This reaction can be expressed as:

$$\text{Chromite} + Na^{+}_{(aq)} + Al^{3+}_{(aq)} + Si^{4+}_{(aq)} \rightarrow \text{Kosmochlor} + \text{Cr-jadeite}.$$

A chromite–kosmochlor–Cr-omphacite or chromite–Cr-omphacite layered structure is often observed in the amphibolite samples (Figure 4e,f), different from the chromite–kosmochlor–Cr-jadeite layered structure in jadeitite. This kosmochlor is the Jd-Kos-Di ternary join, which differs from the Jd-Kos join in jadeitite. The fluid–rock interaction may have led to $Ca^{2+}_{(aq)}$ and $Mg^{2+}_{(aq)}$ entry from magnesio-katophorite into the Jd-Kos system and the formation of Cr-rich omphacite. The negative correlation between (Na + Cr + Al) and (Ca + Mg) in the kosmochlor and Cr-omphacite (Figure 10) indicates that the coupled substitution of (Na + Cr +Al) by (Ca + Mg) is the dominant mechanism for the incorporation of Cr^{3+} into the octahedral site [28]. From chromite-1 to chromite-3, the Cr content of the surrounding kosmochlor decreases, while the Ca-Mg content increases, and the isomorphic join transitions to the Di end-member until it becomes Cr-omphacite.

The reaction can be expressed as:

$$\text{Chromite} + \text{Magnesio-katophorite} + Na^{+}_{(aq)} + Al^{3+}_{(aq)} + Si^{4+}_{(aq)} \rightarrow \text{Kosmochlor} + \text{Cr-omphacite}.$$

The pyroxene fracture-filling veins formed when the jadeite-forming fluids in the subduction zone infiltrated the magnesio-katophorite along the fractures under high-pressure and low-temperature conditions. The pyroxene grains in the veins were euhedral with rhythmic zoning with pure jadeite core and omphacite rim. The omphacite component in the fracture-filling pyroxene veins was higher than that in the massive pure jadeite formed by large amounts of fluid. This also indicates that the fluid's composition was

altered by a reaction with magnesio-katophorite, which increased the Ca-Mg content of the jadeite-forming fluid.

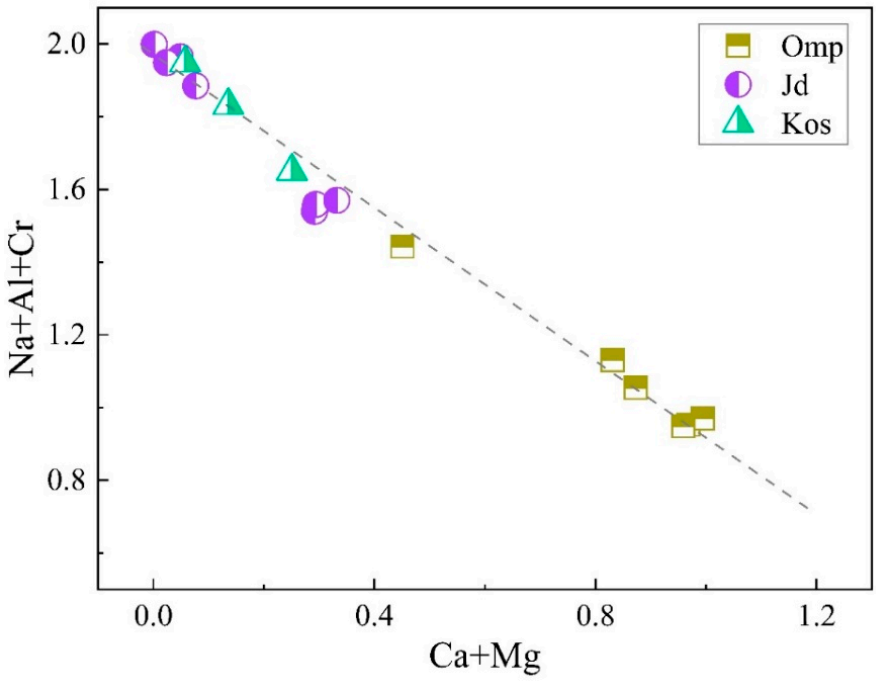

Figure 10. (Na + Cr +Al) vs. (Ca + Mg) (in number of atoms based on 6 O atoms) plot for kosmochlor and Cr-omphacite in the chromite-bearing amphibolite.

5.4. The Proverbial "Moss Spray Green"

In Myanmar's jadeite mines and rough material market, the term "moss spray green" is commonly used. It refers to the intense green color of jadeitite, which is derived from the moss-like appearance of dark green amphibolite.

The chromite-bearing amphibolite may have been broken up by the introduction of a large amount of Na-Al-Si-rich fluid, and the amphibolite pieces may have been wrapped in the fluid and formed jadeitite containing chromite + kosmochlor + Cr-jadeite (Figure 9). Green jadeite was formed by metasomatic action.

This process also explains the proverbial "moss spraying green", where the amphibole brings out the green color in jadeitite. However, it is the chromite in the amphibole that brings out the green color.

6. Conclusions

The residual chromite in amphibolite (magnesio-katophorite) has lower Al-Mg and higher Cr-Mn contents (similar to chromite in green jadeitite) than the adjacent serpentinized peridotite. However, its degree of alteration is generally lower than that in green jadeitite.

Serpentinite is derived from a highly depleted mantle peridotite. There were at least two stages of metasomatism during the transformation of serpentinite+chromite to amphibolite + chromite + kosmochlor. The first stage was the Ca-rich metasomatism of serpentinite, resulting in sodic-calcic amphibole (magnesio-katophorite), which preceded the formation of jadeite. The second stage of Na-rich metasomatism was produced by the Na-Al-Si-rich fluids and the magnesio-katophorite + chromite (contemporaneous with the formation of jadeite). The composition of the fluid was altered by a reaction with magnesio-katophorite, increasing the Ca-Mg content and resulting in the formation of kosmochlor rich in omphacite and/or peripheral Cr-omphacite. This kosmochlor–Cr-omphacite belongs to

the Jd-Kos-Di ternary join, which differs from the kosmochlor–Cr-jadeite (which belongs to the Jd-Kos join in jadeitite).

The formation of jadeitite with chromite + kosmochlor + Cr-jadeite occurs when large amounts of Na-Al-Si-rich fluids have wrapped the pieces of chromite-bearing amphibolite. This conclusion also explains the proverbial "moss spray green", where amphibole (with chromite) brings out the green color in jadeitite.

Supplementary Materials: The following supporting information can be downloaded at: https://www.mdpi.com/article/10.3390/cryst15010079/s1, Table S1: EMPA data (wt.%) and chemical formula calculations for chromite in the amphibolite.; Table S2: EMPA data (wt.%) and chemical formula calculations for pyroxene in the amphibolite; Table S3: EMPA data (wt.%) and chemical formula calculations for magnesio-katophorit in the amphibolite.

Author Contributions: Conceptualization, Y.Z. and G.S.; methodology, Y.Z.; software, J.W.; validation, Y.Z. and J.W.; formal analysis, Y.Z.; investigation, Y.Z. and J.W.; resources, Y.Z. and G.S.; data curation, Y.Z. and J.W.; writing—original draft preparation, Y.Z.; writing—review and editing, Y.Z. and G.S.; visualization, Y.Z.; supervision, G.S.; project administration, G.S.; and funding acquisition, G.S. All authors have read and agreed to the published version of the manuscript.

Funding: This research was funded by the National Natural Science Foundation of China, grant number 42273044.

Data Availability Statement: The data presented in this study are available within the article and Supplementary Materials (including Tables S1–S3).

Acknowledgments: The authors would like to thank Yuan Y. for laboratory technical support (School of Gemology, China University of Geosciences, Beijing).

Conflicts of Interest: The authors declare no conflicts of interest.

References

1. Stern, R.J.; Tsujimori, T.; Harlow, G.; Groat, L.A. Plate tectonic gemstones. *Geology* **2013**, *41*, 723–726. [CrossRef]
2. Mitchell, A.; Htay, M.T.; Htun, K.M. Middle Jurassic arc reversal, Victoria–Katha Block and Sibumasu Terrane collision, jadeite formation and Western Tin Belt generation, Myanmar. *Geol. Mag.* **2021**, *158*, 1487–1503. [CrossRef]
3. Timsina, P.; Hearn, T.M.; Ni, J.F. Crust and mantle flow from Central Tibetan Plateau to the Indo-Burma subduction zone. *J. Geophys. Res. Solid Earth* **2024**, *129*, e2023JB027540. [CrossRef]
4. Shi, G.H.; Cui, W.Y.; Tropper, P.; Wang, C.Q.; Shu, G.-M.; Yu, H. The petrology of a complex sodic and sodic-calcic amphibole association and its implications for the metasomatic processes in the jadeitite area in northwestern Myanmar, formerly Burma. *Contrib. Mineral. Petrol.* **2003**, *145*, 355–376. [CrossRef]
5. Shi, G.H.; Stöckhert, B.; Cui, W.Y. Kosmochlor and chromian jadeite aggregates from the Myanmar jadeitite area. *Mineral. Mag.* **2005**, *69*, 1059–1075. [CrossRef]
6. Shi, G.H.; Cui, W.Y.; Cao, S.M.; Jiang, N.; Jian, P.; Liu, D.Y.; Miao, L.C.; Chu, B.B. Ion microprobe zircon U-Pb age and geochemistry of the Myanmar jadeitite. *J. Geol. Soc.* **2008**, *165*, 221–234. [CrossRef]
7. Shi, G.; Lei, W.; He, H.; Ng, Y.N.; Liu, Y.; Liu, Y.; Yuan, Y.; Kang, Z.; Xie, G. Superimposed tectono-metamorphic episodes of Jurassic and Eocene age in the jadeite uplift, Myanmar, as revealed by 40Ar/39Ar dating. *Gondwana Res.* **2014**, *26*, 464–474. [CrossRef]
8. Morley, C.K.; Naing, T.T.; Searle, M.; Robinson, S.A. Structural and tectonic development of the Indo-Burma ranges. *Earth-Sci. Rev.* **2020**, *200*, 102992. [CrossRef]
9. Zhang, X.; Shi, G.; Li, G.; Li, X. Weathered cortex of eluvial–deluvial jadeite jade from Myanmar: Its features, formation mechanism, and implications. *Minerals* **2022**, *12*, 797. [CrossRef]
10. Liu, C.-Z.; Zhang, C.; Xu, Y.; Wang, J.-G.; Chen, Y.; Guo, S.; Wu, F.-Y.; Sein, K. Petrology and geochemistry of mantle peridotites from the Kalaymyo and Myitkyina ophiolites (Myanmar): Implications for tectonic settings. *Lithos* **2016**, *264*, 495–508. [CrossRef]
11. Chen, Y.; Huang, F.; Shi, G.-H.; Wu, F.-Y.; Chen, X.; Jin, Q.-Z.; Su, B.; Guo, S.; Sein, K.; Nyunt, T.T. Magnesium Isotope Composition of Subduction Zone Fluids as Constrained by Jadeitites from Myanmar. *J. Geophys. Res. Solid Earth* **2018**, *123*, 7566–7585. [CrossRef]
12. Ridd, M.F.; Crow, M.J.; Morley, C.K. The role of strike-slip faulting in the history of the Hukawng Block and the Jade Mines Uplift, Myanmar. *Proc. Geol. Assoc.* **2019**, *130*, 126–141. [CrossRef]

13. Zhang, Y.; Shi, G. Origin of Blue-Water Jadeite Jades from Myanmar and Guatemala: Differentiation by Non-Destructive Spectroscopic Techniques. *Crystals* **2022**, *12*, 1448. [CrossRef]
14. Oberti, R.; Boiocchi, M.; Hawthorne, F.C.; Ball, N.A.; Harlow, G.E. Katophorite from the Jade Mine Tract, Myanmar: Mineral description of a rare (grandfathered) endmember of the amphibole supergroup. *Mineral. Mag.* **2018**, *79*, 355–363. [CrossRef]
15. Shi, G.; Harlow, G.E.; Wang, J.; Wang, J.; Enoch, N.G.; Wang, X.; Cao, S.M.; Enyuancui, W. Mineralogy of jadeitite and related rocks from Myanmar: A review with new data. *Eur. J. Mineral.* **2012**, *24*, 345–370. [CrossRef]
16. Nyunt, T.T. Petrological and Geochemical Contribution to the Origin of Jadeitite and Associated Rocks of the Tawmaw Area, Kachin State, Myanmar. Ph.D. Thesis, University of Stuttgart, Stuttgart, Germany, 2009.
17. Tsujimori, T.; Harlow, G.E. Petrogenetic relationships between jadeitite and associated high-pressure and low-temperature metamorphic rocks in worldwide jadeitite localities: A review. *Eur. J. Mineral.* **2012**, *24*, 371–390. [CrossRef]
18. Shi, G.; Wang, X.; Chu, B.; Cui, W. Jadeite jade from Myanmar: Its texture and gemmological implications. *J. Gemmol.* **2009**, *31*, 185–195. [CrossRef]
19. Sorensen, S.S.; Harlow, G.E.; Rumble, D.I. The origin of jadeitite-forming subduction-zone fluids: CL-guided SIMS oxygen-isotope and trace-element evidence. *Am. Mineral.* **2006**, *91*, 979–996. [CrossRef]
20. Harlow, G.E.; Tsujimori, T.; Sorensen, S.S. Jadeitites and Plate Tectonics. *Annu. Rev. Earth Planet. Sci.* **2015**, *43*, 105–138. [CrossRef]
21. Shi, G.-H.; Jiang, N.; Liu, Y.; Wang, X.; Zhang, Z.-Y.; Xu, Y.-J. Zircon Hf isotope signature of the depleted mantle in the Myanmar jadeitite: Implications for Mesozoic intra-oceanic subduction between the Eastern Indian Plate and the Burmese Platelet. *Lithos* **2009**, *112*, 342–350. [CrossRef]
22. Compagnoni, R.; Rolfo, F.; Castelli, D. Jadeitite from the Monviso meta-ophiolite, western Alps: Occurrence and genesis. *Eur. J. Mineral.* **2012**, *24*, 333–343. [CrossRef]
23. Ng, Y.-N.; Shi, G.-H.; Santosh, M. Titanite-bearing omphacitite from the Jade Tract, Myanmar: Interpretation from mineral and trace element compositions. *J. Asian Earth Sci.* **2016**, *117*, 1–12. [CrossRef]
24. Lei, W.; Shi, G.; Santosh, M.; Ng, Y.; Liu, Y.; Wang, J.; Xie, G.; Ju, Y. Trace element features of hydrothermal and inherited igneous zircon grains in mantle wedge environment: A case study from the Myanmar jadeitite. *Lithos* **2016**, *266–267*, 16–27. [CrossRef]
25. Ouyang, C.M. A terrestrial source of ureyite. *Am. Mineral.* **1984**, *69*, 1180–1183.
26. Mével, C.; Kienast, J.-R. Jadeite-kosmochlor solid solution and chromian sodic amphiboles in jadeitites and associated rocks from Tawmaw (Burma). *Bull. Minér.* **1986**, *109*, 617–633. [CrossRef]
27. Harlow, G.E.; Olds, E.P. Observations on terrestrial ureyite and ureyitic pyroxene. *Am. Mineral.* **1987**, *72*, 126–136.
28. Frondel, C.; Klein, C. Ureyite, $NaCrSi_2O_6$: A New Meteoritic Pyroxene. *Science* **1965**, *149*, 742–744. [CrossRef] [PubMed]
29. Couper, A.G.; Hey, M.H.; Hutchison, R. Cosmochlore—A new examination. *Mineral. Mag.* **1981**, *44*, 265–267. [CrossRef]
30. Sakamoto, S.; Takasu, A. Kosmochlor from the Osayama ultramafic body in the Sangun metamorphic belt, southewest Japan. *J. Geol. Soc. Jpn.* **1996**, *102*, 49–52. [CrossRef]
31. Reznitsky, L.Z.; Sklyarov, E.V.; Galuskin, E.V. Complete isomorphic join diopside–kosmochlor $CaMgSi_2O_6$–$NaCrSi_2O_6$ in metamorphic rocks of the Sludyanka complex (southern Baikal region). *Russ. Geol. Geophys.* **2011**, *52*, 40–51. [CrossRef]
32. Ouyang, C.M.; Qi, L.J. Hte long sein—A new variety of chrome jadeite jade. *J. Gemmol.* **2001**, *27*, 321–327. [CrossRef]
33. Mitchell, A.; Chung, S.-L.; Oo, T.; Lin, T.-H.; Hung, C.-H. Zircon U–Pb ages in Myanmar: Magmatic–metamorphic events and the closure of a neo-Tethys ocean? *J. Asian Earth Sci.* **2012**, *56*, 1–23. [CrossRef]
34. Mitchell, A. Jade Mines—Loimaw Uplift. In *Geological Belts, Plate Boundaries, and Mineral Deposits in Myanma*; Elsevier: Amsterdam, The Netherlands, 2018; pp. 439–460.
35. Searle, M.P.; Noble, S.R.; Cottle, J.M.; Waters, D.J.; Mitchell, A.H.G.; Hlaing, T.; Horstwood, M.S.A. Tectonic evolution of the Mogok metamorphic belt, Burma (Myanmar) constrained by U-Th-Pb dating of metamorphic and magmatic rocks. *Tectonics* **2007**, *26*, TC3014. [CrossRef]
36. Searle, M.P.; Palin, R.M.; Gardiner, N.J.; Htun, K.; Wade, J. The Burmese Jade Mines belt: Origins of jadeitites, serpentinites, and ophiolitic peridotites and gabbros. *J. Geol. Soc.* **2023**, *180*, jgs2023-004. [CrossRef]
37. Oberti, R.; Boiocchi, M.; Hawthorne, F.C.; Ball, N.A.; Harlow, G.E. Eckermannite revised: The new holotype from the Jade Mine Tract, Myanmar—Crystal structure, mineral data, and hints on the reasons for the rarity of eckermannite. *Am. Mineral.* **2015**, *100*, 909–914. [CrossRef]
38. Harlow, G.; Sisson, V.; Sorensen, S. Jadeitite from Guatemala: New observations and distinctions among multiple occurrences. *Geol. Acta* **2011**, *9*, 363–387.
39. Skelton, R.; Walker, A.M. The effect of cation order on the elasticity of omphacite from atomistic calculations. *Phys. Chem. Miner.* **2015**, *42*, 677–691. [CrossRef]
40. Flores, K.E.; Martens, U.C.; Harlow, G.E.; Brueckner, H.K.; Pearson, N.J. Jadeitite formed during subduction: In situ zircon geochronology constraints from two different tectonic events within the Guatemala Suture Zone. *Earth Planet. Sci. Lett.* **2013**, *371–372*, 67–81. [CrossRef]
41. Morimoto, N. Nomenclature of Pyroxenes. *Mineral. Petrol.* **1988**, *39*, 55–76. [CrossRef]

42. Ouyang, C.M.; Ng, M. Nomenclature and classification of Fei Cui (pyroxene jade). In Proceedings of the 3rd International Gem and Jewelry Conference (GIT 2012), Bangkok, Thailand, 12–16 December 2012.
43. Leake, B.E.; Woolley, A.R.; Arps, C.E.S.; Birch, W.D.; Gilbert, M.C.; Grice, J.D.; Hawthorne, F.C.; Kato, A.; Kisch, H.J.; Krivovichev, V.G.; et al. Nomenclature of amphiboles; Report of the Subcommittee on Amphiboles of the International Mineralogical Association, Commission on New Minerals and Mineral Names. *Am. Mineral.* **1997**, *82*, 1019–1037.
44. Manning, C.E. Fluid composition at the blueschist-eclogite transition in the model system Na_2O-MgO-Al_2O_3-SiO_2-H_2O-HCl, Swiss Bull. *Miner. Pet.* **1998**, *78*, 225–242.
45. Shi, G.H.; Zhu, X.K.; Deng, J.; Mao, Q.; Liu, Y.X.; Li, G.W. Spherules with pure iron cores from Myanmar jadeitite: Type-I deep-sea spherules? *Geochim. Cosmochim. Acta* **2011**, *75*, 1608–1620. [CrossRef]
46. Qiu, Z.; Wu, F.; Yang, S.; Zhu, M.; Sun, J.; Yang, P. Age and genesis of the Myanmar jadeite: Constraints from U-Pb ages and Hf isotopes of zircon inclusions. *Chin. Sci. Bull.* **2009**, *54*, 658–668. [CrossRef]
47. Kobayashi, S.; Miyake, H.; Shoji, T. A Jadeite Rock from Oosa-cho, Okayama Prefecture, Southwestern Japan. *Mineral. J.* **1987**, *13*, 314–327. [CrossRef]
48. Harlow, G.E. Jadeitites, albitites and related rocks from the Motagua Fault Zone, Guatemala. *J. Metamorph. Geol.* **1994**, *12*, 49–68. [CrossRef]
49. Miyajima, H.; Matsubara, S.; Miyawaki, R.; Ito, K. Itoigawaite, a new mineral, the Sr analogue of lawsonite, in jadeitite from the Itoigawa-Ohmi District, central Japan. *Mineral. Mag.* **1999**, *63*, 909–916. [CrossRef]
50. Morishita, T. Occurrence and chemical composition of barian feldspars in a jadeitite from the Itoigawa-Ohmi district in the Renge high-P/T-type metamorphic belt, Japan. *Mineral. Mag.* **2005**, *69*, 39–51. [CrossRef]
51. Shi, G.; Jiang, N.; Wang, Y.; Zhao, X.; Wang, X.; Li, G.; Ng, E.; Cui, W. Ba minerals in clinopyroxene rocks from the Myanmar jadeitite area: Implications for Ba recycling in subduction zones. *Eur. J. Mineral.* **2010**, *22*, 199–214. [CrossRef]
52. Simons, K.K.; Harlow, G.E.; Brueckner, H.K.; Goldstein, S.L.; Sorensen, S.S.; Hemming, N.G.; Langmuir, C.H. Lithium isotopes in Guatemalan and Franciscan HP–LT rocks: Insights into the role of sediment-derived fluids during subduction. *Geochim. Cosmochim. Acta* **2010**, *74*, 3621–3641. [CrossRef]
53. Wohlers, A.; Manning, C.E.; Thompson, A.B. Experimental investigation of the solubility of albite and jadeite in H_2O, with paragonite+quartz at 500 and 600 °C, and 1–2.25 GPa. *Geochim. Cosmochim. Acta* **2011**, *75*, 2924–2939. [CrossRef]
54. Wang, X.; Shi, G.H.; Qiu, D.F.; Wang, J.; Cui, W.Y. Grossular-bearing jadeite omphacite rock in the Myanmar jadeite area: A kind of jadeitized rodingite? *Eur. J. Mineral.* **2012**, *24*, 237–246. [CrossRef]
55. Harlow, G.E.; Flores, K.E.; Marschall, H.R. Fluid-mediated mass transfer from a paleosubduction channel to its mantle wedge: Evidence from jadeitite and related rocks from the Guatemala Suture Zone. *Lithos* **2016**, *258–259*, 15–36. [CrossRef]
56. Cárdenas-Párraga, J.; García-Casco, A.; Harlow, G.E.; Blanco-Quintero, I.F.; Agramonte, Y.R.; Kröner, A. Hydrothermal origin and age of jadeitites from Sierra del Convento Mélange (Eastern Cuba). *Eur. J. Mineral.* **2012**, *24*, 313–331. [CrossRef]
57. Cárdenas-Párraga, J.; Garcia-Casco, A.; Blanco-Quintero, I.F.; Rojas-Agramonte, Y.; Cambra, K.N.; Harlow, G.E. A highly dynamic hot hydrothermal system in the subduction environment: Geochemistry and geochronology of jadeitite and associated rocks of the Sierra del Convento mélange (eastern Cuba). *Am. J. Sci. Arts* **2021**, *321*, 822–887. [CrossRef] [PubMed]
58. Angiboust, S.; Glodny, J.; Cambeses, A.; Raimondo, T.; Monié, P.; Popov, M.; Garcia-Casco, A. Drainage of subduction interface fluids into the forearc mantle evidenced by a pristine jadeitite network (Polar Urals). *J. Metamorph. Geol.* **2020**, *39*, 473–500. [CrossRef]
59. Reynard, B.; Ballèvre, M. Coexisting amphiboles in an eclogite from the Western Alps: New constraints on the miscibility gap between sodic and calcic amphiboles. *J. Metamorph. Geol.* **1988**, *6*, 333–350. [CrossRef]
60. Kaeser, B.; Kalt, A.; Pettke, T. Crystallization and Breakdown of Metasomatic Phases in Graphite-bearing Peridotite Xenoliths from Marsabit (Kenya). *J. Petrol.* **2007**, *48*, 1725–1760. [CrossRef]
61. Ali, M.; Arai, S. Cr-rich magnesiokatophorite as an indicator of mantle metasomatism by hydrous Na-rich carbonatite. *J. Mineral. Petrol. Sci.* **2013**, *108*, 215–226. [CrossRef]
62. Qi, L.J.; Zheng, S.; Pei, J.C. Mechanism for kosmochlor symplectite and compositional variation zoning in jadeite jade. *J. Gems. Gemmol.* **1999**, *1*, 13–17. (In Chinese with English Abstract)